

# Research Journal of Pharmaceutical, Biological and Chemical Sciences

## Homotrimetallic transition metal complexes of 2-hydroxy-N<sup>1</sup>,N<sup>2</sup>,N<sup>3</sup>-triphenylpropane-1,2,3-tricarbohydrazide preparation, characterization and microbeside activities.

Mohamad M. E. Shakdofa<sup>1,2\*</sup>, Majed H. Shtaiwi<sup>3</sup>, Nagy Morsy<sup>1,4</sup>, and Anas Rasras<sup>1</sup>.

<sup>1</sup>Chemistry Department, Faculty of Sciences and Arts, Khulais, University of Jeddah, Saudi Arabia

<sup>2</sup>Inorganic Chemistry Department, National Research Centre, Elbehothe st., P.O. 12622, Dokki, Cairo, Egypt

<sup>3</sup>Chemistry Department, the Hashemite University, Zarqa, Jordan

<sup>4</sup>Chemistry of Natural Compounds, National Research Centre, Elbehothe st., P.O. 12622, Dokki, Cairo, Egypt

### ABSTRACT

Homotrimetallic Cu(II), Co(II), Ni(II) and Fe(III) Complexes of N<sup>1</sup>,N<sup>2</sup>,N<sup>3</sup>-triphenylpropane-1,2,3-tricarbohydrazide were prepared and analytically and spectroscopically characterized. The ligand was found to be acted as neutral or tribasic hexadentate N<sub>3</sub>O<sub>3</sub> ligand bonded covalency or coordinatively via the carbonyl oxygen of carboxylate moieties in ketonic or enolic and amino nitrogen atoms. Distorted octahedral, tetrahedral or square planar geometries around the metal ions were proved by magnetic and electronic spectra measurements. The antimicrobial screening tests by Well diffusion method revealed that all complexes are biologically more active than the parent ligand and they are more active against Fungus *A. niger* than bacteria *E. coli* and *K. pneumonia*.

**Keywords:** Homotrimetallic complexes, hexadentate, antimicrobial, hydrazone, tricarbohydrazide

\*Corresponding author

## INTRODUCTION

The interaction of transition metal ions with biologically active ligands provides one of the most wonderful areas of coordination chemistry because it enhances their activities. Recent years witnessed an intensive investigation of the coordination chemistry of poly-metallic metal complexes, which are very important class of these compounds due to their potential applications of some of these compounds in different areas. Among these are their using as catalysts[1-2], semiconductors[3-4], luminescent systems[5-6], material for electronic devices[7], molecular-based magnetic materials[8-9] as well as to mimic metalloenzymes active site[10-11]. They sever in transport processes and modelling of several biological compounds [12-15].skeleton of ligands that contain nitrogen–oxygen donors have been studied intensively to understand and reproduce the catalytic activity of metallo-enzyme and to simulate the natural carriers function in recognizing and transporting of specific molecules or ions[16].The multidentate ligands have several chelating sites with *o*-hydroxy aromatic aldehydes, ketones, azomethine and amide, which are able to form multimetallic complexes with suitable transition metals. They show promising importance in the bioinorganic chemistry field[17], chemical reactivity and molecular magnets[18]. Metal-ligand bonding in such complexes involves *r/p* electrons of *o*-hydroxy aromatic aldehydes and ketones[17]. This work aimed for preparation and characterization of new polydentate ligand namely, 2-hydroxy- $N^1, N^2, N^3$ -triphenylpropane-1,2,3-tricarbohydrazide ( $H_3L$ ). The prepared ligand has a potential activity towards complexation and so the study extended to prepare its Cu(II), Ni(II), Co(II), manganese(II), and Fe(III) complexes. The ligand and its complexes were characterized using several techniques such as IR, MS, NMR, UV. Vis, elemental, magnetic moment and thermal measurements. The bioactivity of prepared compounds was studied against *E. coli*, *K. pneumoniae* and *A. niger* using Well Diffusion Method.

## MATERIALS AND METHODS

All the reagents employed for the preparation of the ligands and their complexes were of the analytical grade and used without further purification. 1,5-dimethyl-3-oxo-2-phenylpyrazole-4-carbaldehyde was provided from [Toronto Research Chemicals](#). DMSO (assay 99.7%). absolute ethanol (assay  $\geq 99.8\%$ ). Metal salts were provided from SIGMA-ALDRICH company;  $CuCl_2$ ,  $Cu(NO_3)_2 \cdot 3H_2O$ ,  $CuSO_4 \cdot 5H_2O$ ,  $CoCl_2 \cdot 6H_2O$ ,  $Co(NO_3)_2 \cdot 6H_2O$ ,  $CoSO_4 \cdot 7H_2O$ ,  $NiCl_2 \cdot 6H_2O$ ,  $Ni(NO_3)_2 \cdot 6H_2O$ ,  $NiSO_4 \cdot 6H_2O$ ,  $FeCl_3 \cdot 6H_2O$ ,  $Fe_2(NO_3)_3 \cdot 9H_2O$ , triethyl amine (TEA) with purity from 98 to 99.99%.

### Instrumentation and measurements

The ligand and its metal complexes were analyzed for C, H, N, Cl and S at the Micro-analytical Laboratory, Cairo University, Egypt. Triethyl 2-hydroxypropane-1,2,3-tricarboxylate was prepared according to a known method. Standard analytical methods were used to determine the metal ion content[53-56].IR spectra of the ligand and its metal complexes were measured with using a Jasco FT/IR 300E Fourier transform infrared spectrophotometer covering the range  $400-4000\text{ cm}^{-1}$ . Nujol mull electronic spectra were recorded using Whatman filter paper No.1 and referenced against another similar filter paper saturated with paraffin oil in the 200-1100 nm regions on a SHMADZU 2600 spectrophotometer. The thermal analysis (TG) was carried out on Shimadzu DT-30 thermal analyzer from room temperature to  $800\text{ }^\circ\text{C}$  at a heating rate of  $10\text{ }^\circ\text{C}/\text{min}$ . Magnetic susceptibilities were measured at  $25^\circ\text{C}$  by the Gouy method using mercuric tetrathiocyanatocobaltate(II) as the magnetic susceptibility standard. Diamagnetic corrections were estimated from Pascal's constant[57].The magnetic moments were calculated from the equation (1):

$$\mu_{\text{eff}} = 2.84 \sqrt{\chi_M^{\text{corr}} \cdot T} \quad (1)$$

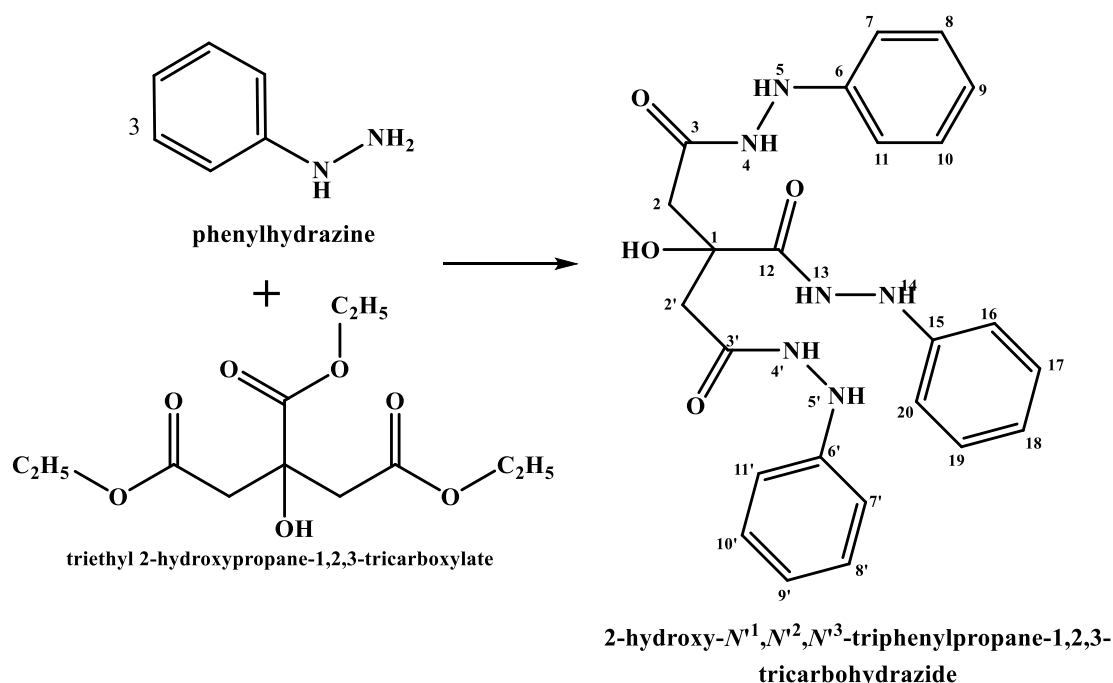
Molar conductance were measured on a Tacussel type  $CD_6NG$  conductivity bridge using  $10^{-3}\text{ M}$  DMF solutions. The resistance measured in ohms and the molar conductivities were calculated according to the equation (2):

$$\Lambda_M = \frac{V \times K \times g}{Mw \times \Omega} \quad (2) \text{ Where: } \Lambda_M = \text{molar conductivity} / \Omega^{-1} \text{ cm}^2 \text{ mol}^{-1}, V = \text{volume of the complex solution} / \text{mL}, K = \text{cell constant} (0.92 / \text{cm}^{-1}), Mw = \text{molecular weight of the complex}, g = \text{weight of the complex in gram}, \Omega = \text{resistance. NMR spectrum was obtained on Bruker Avance 600-DRX spectrometers. Mass spectra of the solid}$$

ligand and its metal complexes recorded using JEUL JMS-AX-500 mass spectrometer provided with data system. TLC confirmed the purity of all prepared compounds.

### Preparation of carbohydraide ligand (H<sub>3</sub>L)

The 2-hydroxy-*N*<sup>1</sup>,*N*<sup>2</sup>,*N*<sup>3</sup>-triphenylpropane-1,2,3-tricarbohydraide ligand was prepared by refluxing triethyl 2-hydroxypropane-1,2,3-tricarboxylate (276 mg, 1 mmol) dissolved in 50 cm<sup>3</sup> of methanol with phenyl hydrazine (3.24 g, 3 mmol) dissolved in 50 cm<sup>3</sup> of methanol [Scheme 1]. The mixture refluxed for four hours with stirring. After cooling, the formed solid product filtered off, then washed several times with cold methanol and finally dried at room temperature over P<sub>4</sub>O<sub>10</sub>. Yield (308 mg, 66.6%), color is buff, m.p. 210 °C, Elemental analysis for C<sub>24</sub>H<sub>26</sub>N<sub>6</sub>O<sub>4</sub> (462.51): Found (calcd) %C 61.97 (62.33), %H 5.33 (5.67), %N 18.13 (18.17). IR (KBr, cm<sup>-1</sup>), 3323, 3288, 3265 ν(NH), 1698, 1683, 1655 ν(C=O). <sup>1</sup>H-NMR (600 MHz, DMSO-*d*<sub>6</sub>): 6.04 (s, 1 H, <sup>21</sup>O-H), 9.81 (s, 1 H, <sup>4</sup>N-H), 7.72 (s, 1 H, <sup>5</sup>N-H), 9.68 (s, 1 H, <sup>4'</sup>N-H), 7.57 (s, 1H, <sup>5'</sup>N-H), 9.75 (s, 1H, <sup>13</sup>N-H), 7.52 (1H, <sup>14</sup>N-H), 6.77 (6 H, <sup>7</sup>C-H, <sup>11</sup>C-H, <sup>7'</sup>C-H, <sup>11'</sup>C-H, <sup>16</sup>C-H & <sup>20</sup>C-H), 7.13 (6 H, <sup>8</sup>C-H, <sup>10</sup>C-H, <sup>8'</sup>C-H, <sup>10'</sup>C-H, <sup>17</sup>C-H & <sup>19</sup>C-H), 6.71 (3 H, <sup>9</sup>C-H, <sup>9'</sup>C-H & <sup>18</sup>C-H), 2.73 (s, 2 H, <sup>2</sup>C-H<sub>2</sub>), 2.75 (s, 2 H, <sup>2'</sup>C-H<sub>2</sub>). <sup>13</sup>C-NMR (600 Mhz, DMSO-*d*<sub>6</sub>): 75.22 (C1), 41.12 (C2), 170.34 (C3), 149.52 (C6), 112.76 (C7), 129.01(C8), 118.97(C9), 129.01(C10), 112.76(C11), 41.12 (C2'), 170.34 (C3'), 149.52 (C6'), 112.76 (C7'), 129.01(C8'), 118.97(C9'), 129.01(C10'), 112.76(C11'), 173.95 (C12), 149.52 (C15), 112.76 (C16), 129.01 (C17), 118.97 (C19), 129.01 (C20).



**Scheme 1:** Synthesis of the ligand 2-hydroxy-*N*<sup>1</sup>,*N*<sup>2</sup>,*N*<sup>3</sup>-triphenylpropane-1,2,3-tricarbohydraide

### Preparation of homotrimetallic metal complexes (2-12)

The complexes (2-12) were prepared by adding metal salts CuCl<sub>2</sub>, Cu(NO<sub>3</sub>)<sub>2</sub>·3H<sub>2</sub>O, CuSO<sub>4</sub>·5H<sub>2</sub>O, CoCl<sub>2</sub>·6H<sub>2</sub>O, Co(NO<sub>3</sub>)<sub>2</sub>·6H<sub>2</sub>O, CoSO<sub>4</sub>·7H<sub>2</sub>O, NiCl<sub>2</sub>·6H<sub>2</sub>O, Ni(NO<sub>3</sub>)<sub>2</sub>·6H<sub>2</sub>O, NiSO<sub>4</sub>·6H<sub>2</sub>O, FeCl<sub>3</sub>·6H<sub>2</sub>O, Fe<sub>2</sub>(NO<sub>3</sub>)<sub>3</sub>·9H<sub>2</sub>O (3 mmol, in 50 mL of ethanol) to 2-hydroxy-*N*<sup>1</sup>,*N*<sup>2</sup>,*N*<sup>3</sup>-triphenylpropane-1,2,3-tricarbohydraide ligand (H<sub>3</sub>L) (462 mg, 1 mmol, in 50 mL of absolute ethanol) in the presence of 3 ml of triethylamine. The mixture refluxed for Six hours with stirring. The resulting solid complexes filtered off while heated, washed several times with hot ethanol and finally dried over P<sub>4</sub>O<sub>10</sub>.

**Complex (2):** Yield (56.6%), m.p. >300 °C; color: brown; μ<sub>eff</sub> = 1.29; molar conductivity (Λ<sub>m</sub>): 23.1 ohm<sup>-1</sup>cm<sup>2</sup>mol<sup>-1</sup> Elemental analysis for [Cu<sub>3</sub>(L)(Cl)<sub>3</sub>(H<sub>2</sub>O)<sub>6</sub>], C<sub>24</sub>H<sub>26</sub>N<sub>6</sub>O<sub>10</sub>Cu<sub>3</sub>Cl<sub>3</sub>, (864.56): Found (calcd) %C 32.99 (33.34), %H 3.85 (4.08), %N 9.21 (9.71), %Cl 12.30 (11.89), %Cu 21.69(22.05). IR (KBr, cm<sup>-1</sup>), 3390, 3270 ν(OH/H<sub>2</sub>O), 1595 ν(C=N), 544 ν(Cu-O), 470 (Cu←N).

**Complex (3):** Yield (63.3%), m.p. = 270 °C; color: olive;  $\mu_{\text{eff}} = 1.34$ ; molar conductivity ( $\Lambda_m$ ):  $19.9 \text{ ohm}^{-1}\text{cm}^2\text{mol}^{-1}$  Elemental analysis for  $[\text{Cu}_3(\text{H}_3\text{L})(\text{NO}_3)_6(\text{H}_2\text{O})_6]$ ,  $\text{C}_{24}\text{H}_{38}\text{N}_{12}\text{O}_{28}\text{Cu}_3$ , (1133.26): Found (calcd) %C 24.98 (25.44), %H 3.13 (3.38), %N 24.66 (24.83) %Cu 15.97(16.82). IR (KBr,  $\text{cm}^{-1}$ ), 3382, 3219  $\nu(\text{OH}/\text{H}_2\text{O})$ , 1632  $\nu(\text{C}=\text{O})$ , 519  $\nu(\text{Cu}-\text{O})$ , 490  $\nu(\text{Cu}-\text{N})$ ,  $\nu_5(\text{NO}_3)$ ,  $\nu_1(\text{NO}_3)$ ,  $\nu_2(\text{NO}_3)$  1454, 1391, 901 ( $\Delta(\nu_5-\nu_1) = 63 \text{ cm}^{-1}$ ).

**Complex (4):** Yield (51.9%), m.p. = 295 °C; color: green;  $\mu_{\text{eff}} = 1.51$ ; molar conductivity ( $\Lambda_m$ ):  $29.5 \text{ ohm}^{-1}\text{cm}^2\text{mol}^{-1}$  Elemental analysis for  $[\text{Cu}_3(\text{H}_3\text{L})(\text{SO}_4)_3(\text{H}_2\text{O})_3]$ ,  $\text{C}_{24}\text{H}_{32}\text{N}_6\text{O}_{19}\text{Cu}_3\text{S}_3$ , (995.36): Found (calcd) %C 29.15 (28.96), %H 3.05 (3.24), %N 8.09 (8.44), %S 9.21 (9.66), %Cu 18.89(19.15). IR (KBr,  $\text{cm}^{-1}$ ), 3570, 3484, 3382  $\nu(\text{OH}/\text{H}_2\text{O})$ , 1628  $\nu(\text{C}=\text{O})$ , 530  $\nu(\text{Cu}-\text{O})$ , 494  $\nu(\text{Cu}-\text{N})$ ,  $\nu_3(\text{SO}_4)$  1147, 1045,  $\nu_4(\text{SO}_4)$  966, 510  $\nu_1(\text{SO}_4)$  630,  $\nu_2(\text{SO}_4)$  594.

**Complex (5):** Yield (61.00%), m.p. >300 °C; color: dark brown;  $\mu_{\text{eff}} = 1.93$ ; molar conductivity ( $\Lambda_m$ ):  $24 \text{ ohm}^{-1}\text{cm}^2\text{mol}^{-1}$  Elemental analysis for  $[\text{Co}_3(\text{L})(\text{Cl})_3(\text{H}_2\text{O})_9].4\text{H}_2\text{O}$ ,  $\text{C}_{24}\text{H}_{47}\text{N}_6\text{O}_{16}\text{Co}_3\text{Cl}_3$ , (976.83): Found (calcd) %C 29.88 (29.51), %H 5.47 (5.06), %N 7.99 (8.60), %Cl 10.77 (10.89), %Co 17.56(18.10). IR (KBr,  $\text{cm}^{-1}$ ), 3330, 3234  $\nu(\text{OH}/\text{H}_2\text{O})$ , 1561  $\nu(\text{C}=\text{N})$ , 502  $\nu(\text{Co}-\text{O})$ , 476  $\nu(\text{Co}-\text{N})$ .

**Complex (6):** Yield (49.4%), m.p. > 300 °C; color: dark brown;  $\mu_{\text{eff}} = 2.16$ ; molar conductivity ( $\Lambda_m$ ):  $18.4 \text{ ohm}^{-1}\text{cm}^2\text{mol}^{-1}$  Elemental analysis for  $[\text{Co}_3(\text{L})(\text{NO}_3)_3(\text{H}_2\text{O})_3]$ ,  $\text{C}_{24}\text{H}_{29}\text{N}_9\text{O}_{16}\text{Co}_3$ , (876.34): Found (calcd) %C 32.08 (32.89), %H 3.23 (3.34), %N 14.40 (14.39) %Co 19.77(20.17). IR (KBr,  $\text{cm}^{-1}$ ), 3395, 3233  $\nu(\text{OH}/\text{H}_2\text{O})$ , 1568  $\nu(\text{C}=\text{N})$ , 503  $\nu(\text{Co}-\text{O})$ , 460  $\nu(\text{Co}-\text{N})$ ,  $\nu_5(\text{NO}_3)$ ,  $\nu_1(\text{NO}_3)$ ,  $\nu_2(\text{NO}_3)$  1457, 1367, 918 ( $\Delta(\nu_5-\nu_1) = 90 \text{ cm}^{-1}$ ).

**Complex (7):** Yield (58.3%), m.p. = 273 °C; color: dark brown;  $\mu_{\text{eff}} = 2.33$ ; molar conductivity ( $\Lambda_m$ ):  $15.0 \text{ ohm}^{-1}\text{cm}^2\text{mol}^{-1}$  Elemental analysis for  $[\text{Co}_3(\text{H}_3\text{L})(\text{SO}_4)_3]$ ,  $\text{C}_{24}\text{H}_{26}\text{N}_6\text{O}_{16}\text{Co}_3\text{S}_3$ , (927.48): Found (calcd) %C 30.55 (31.08), %H 3.01 (2.83), %N 8.67 (9.06), %S 9.97 (10.37), %Co 18.68(19.09). IR (KBr,  $\text{cm}^{-1}$ ), 3371, 3210  $\nu(\text{OH}/\text{H}_2\text{O})$ , 1635  $\nu(\text{C}=\text{O})$ , 528  $\nu(\text{Co}-\text{O})$ , 482  $\nu(\text{Co}-\text{N})$ ,  $\nu_3(\text{SO}_4)$  1240, 1115, 1038,  $\nu_4(\text{SO}_4)$  631, 610, 588  $\nu_1(\text{SO}_4)$  1000,  $\nu_2(\text{SO}_4)$  500.

**Complex (8):** Yield (59.10%), m.p. >300 °C; color: brown;  $\mu_{\text{eff}} = 2.49$ ; molar conductivity ( $\Lambda_m$ ):  $20.3 \text{ ohm}^{-1}\text{cm}^2\text{mol}^{-1}$  Elemental analysis for  $[\text{Ni}_3(\text{L})(\text{Cl})_3(\text{H}_2\text{O})_9]$ ,  $\text{C}_{24}\text{H}_{41}\text{N}_6\text{O}_{13}\text{Ni}_3\text{Cl}_3$ , (904.05): Found (calcd) %C 31.05 (31.89), %H 4.57 (4.39), %N 9.30 (9.46), %Cl 11.29 (11.76), %Ni 18.74(19.48). IR (KBr,  $\text{cm}^{-1}$ ), 3551, 3354, 3234  $\nu(\text{OH}/\text{H}_2\text{O})$ , 1557  $\nu(\text{C}=\text{N})$ , 534  $\nu(\text{Ni}-\text{O})$ , 477  $\nu(\text{Ni}-\text{N})$ .

**Complex (9):** Yield (50.5%), m.p. = 290 °C; color: dark brown;  $\mu_{\text{eff}} = 1.86$ ; molar conductivity ( $\Lambda_m$ ):  $17.8 \text{ ohm}^{-1}\text{cm}^2\text{mol}^{-1}$  Elemental analysis for  $[\text{Ni}_3(\text{L})(\text{NO}_3)_3(\text{H}_2\text{O})_3]$ ,  $\text{C}_{24}\text{H}_{29}\text{N}_9\text{O}_{16}\text{Ni}_3$ , (875.62): Found (calcd) %C 32.09 (32.92), %H 3.34 (3.37), %N 13.86 (14.14) %Ni 19.64(20.11). IR (KBr,  $\text{cm}^{-1}$ ), 3395, 3167  $\nu(\text{OH}/\text{H}_2\text{O})$ , 1575  $\nu(\text{C}=\text{N})$ , 575  $\nu(\text{Ni}-\text{O})$ , 500  $\nu(\text{Ni}-\text{N})$ ,  $\nu_5(\text{NO}_3)$ ,  $\nu_1(\text{NO}_3)$ ,  $\nu_2(\text{NO}_3)$  1457, 1361, 921 ( $\Delta(\nu_5-\nu_1) = 96 \text{ cm}^{-1}$ ).

**Complex (10):** Yield (57.6%), m.p. = 280 °C; color: brown;  $\mu_{\text{eff}} = 1.67$ ; molar conductivity ( $\Lambda_m$ ):  $13.7 \text{ ohm}^{-1}\text{cm}^2\text{mol}^{-1}$  Elemental analysis for  $[\text{Ni}_3(\text{H}_3\text{L})(\text{SO}_4)_3]$ ,  $\text{C}_{24}\text{H}_{26}\text{N}_6\text{O}_{16}\text{Ni}_3\text{S}_3$ , (926.76): Found (calcd) %C 30.75 (31.10), %H 2.77 (2.83), %N 8.99 (9.07), %S 9.83 (10.38), %Ni 18.19(19.00). IR (KBr,  $\text{cm}^{-1}$ ), 3391, 3201  $\nu(\text{OH}/\text{H}_2\text{O})$ , 1597  $\nu(\text{C}=\text{N})$ , 530  $\nu(\text{Ni}-\text{O})$ , 473  $\nu(\text{Ni}-\text{N})$ ,  $\nu_3(\text{SO}_4)$  1231, 1100, 1032,  $\nu_4(\text{SO}_4)$  641, 619, 590  $\nu_1(\text{SO}_4)$  994,  $\nu_2(\text{SO}_4)$  490.

**Complex (11):** Yield (48.7%), m.p. =250 °C; color: dark brown;  $\mu_{\text{eff}} = 4.45$ ; molar conductivity ( $\Lambda_m$ ):  $27.3 \text{ ohm}^{-1}\text{cm}^2\text{mol}^{-1}$  Elemental analysis for  $[\text{Fe}_3(\text{L})(\text{Cl})_6(\text{H}_2\text{O})_6]$ ,  $\text{C}_{24}\text{H}_{35}\text{N}_6\text{O}_{10}\text{Fe}_3\text{Cl}_6$ , (947.81): Found (calcd) %C 29.94 (30.41), %H 3.81 (3.72), %N 8.60 (8.87), %Cl 21.56 (21.66), %Fe 16.89(17.68). IR (KBr,  $\text{cm}^{-1}$ ), 3363, 3201  $\nu(\text{OH}/\text{H}_2\text{O})$ , 1597  $\nu(\text{C}=\text{N})$ , 553  $\nu(\text{Fe}-\text{O})$ , 453  $\nu(\text{Fe}-\text{N})$ .

**Complex (12):** Yield (51.2%), m.p. = 265 °C; color: dark brown;  $\mu_{\text{eff}} = 4.89$ ; molar conductivity ( $\Lambda_m$ ):  $30.31 \text{ ohm}^{-1}\text{cm}^2\text{mol}^{-1}$  Elemental analysis for  $[\text{Fe}_3(\text{L})(\text{NO}_3)_6(\text{H}_2\text{O})_6]$ ,  $\text{C}_{24}\text{H}_{35}\text{N}_{12}\text{O}_{28}\text{Fe}_3$ , (1107.14): Found (calcd) %C 25.37 (26.04), %H 3.03 (3.19), %N 14.53 (15.18) %Fe 14.90(15.13). IR (KBr,  $\text{cm}^{-1}$ ), 3420, 3290  $\nu(\text{OH}/\text{H}_2\text{O})$ , 1588  $\nu(\text{C}=\text{N})$ , 561  $\nu(\text{Fe}-\text{O})$ , 501  $\nu(\text{Fe}-\text{N})$ ,  $\nu_5(\text{NO}_3)$ ,  $\nu_1(\text{NO}_3)$ ,  $\nu_2(\text{NO}_3)$  1435, 1361, 914 ( $\Delta(\nu_5-\nu_1) = 74 \text{ cm}^{-1}$ ).

### Biological activity

In vitro antibacterial and antifungal assays were performed by well diffusion method in the Lab. of microbiology, Biology Department, Faculty of Science and Arts, University of Jeddah, KSA[58-61]. Both positive (nystatin for fungi, Amoxicillin for bacteria) and negative (solvent, DMSO) controls were used in the technique. The complexes and ligand were tested against fungi such as *Aspergillus niger*(A. niger) and bacteria like

*Escherichia coli* (*E. coli*) and *Klebsiella pneumoniae* (*K. pneumonia*) cultured on Czapek Dox's agar and nutrient agar as medium respectively. In a typical procedure, a well was made on the agar medium inoculated with the fungi or bacteria. The well was filled with the test solution (20 mg\ mL) using a micropipette and the plate was incubated at 28 and 37 °C respectively for 72 h. During this period, the test solution diffused and the growth of the inoculated fungi or bacteria was affected. The inhibition zone (MIZ) developed on the plate was measured. Each test was carried out for three times to minimize the error. The activity index for the complexes was calculated by following formula.

$$\text{Activity index} = \frac{\text{Diameter of inhibition zone by test compound}}{\text{Diameter of inhibition zone by standard}} \times 100$$

## RESULTS AND DISCUSSION

The 2-hydroxy-N<sup>1</sup>,N<sup>2</sup>,N<sup>3</sup>-triphenylpropane-1,2,3-tricarbohydrazide (H<sub>3</sub>L), [Scheme 1] and its metal complexes (2)-(12) are stable at room temperature. The complexes were found to be not soluble in ethanol, acetone water and chloroform but soluble in DMSO and DMF. The elemental analysis revealed that the complexes are formed in molar ratios 3 metal: 1 ligand. Unfortunately, attempts were failed to grow single crystal. The analytical, physical and spectral data are presented in experimental part and Table 1-2 and were found to be compatible with the suggested structures [Figs 1-2].

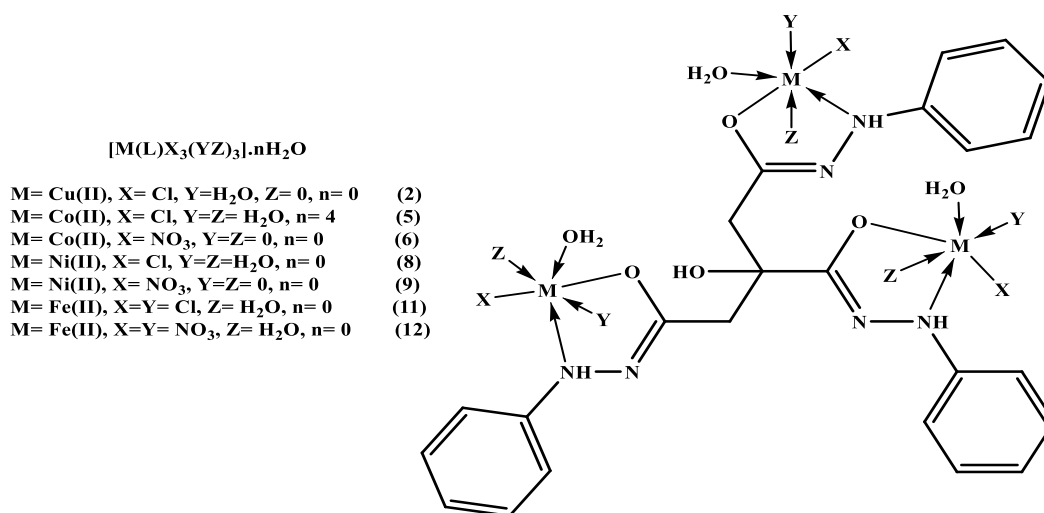


Fig 1: The structure representation of metal complexes (2), (5-6), (8-9) and (11-12)

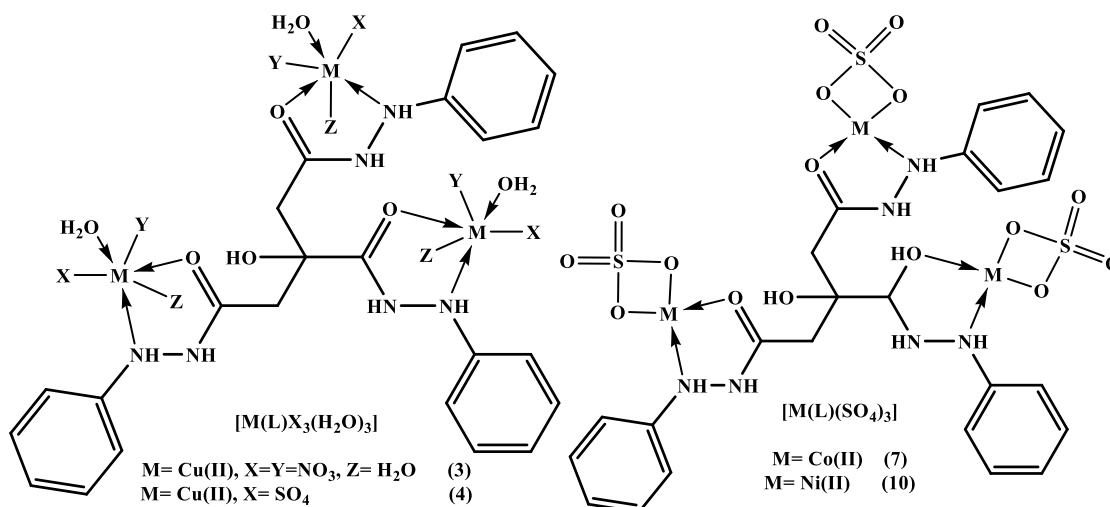


Fig 2: The structure representation of metal complexes (3-4), (7) and (10)

## NUCLEAR MAGNETIC RESONANCE STUDIES

### 1D NMR spectrum

Detailed analysis of  $^1\text{D}$  such as  $^1\text{H}$  NMR and DEPT (90, 135) revealed that ligand ( $\text{H}_3\text{L}$ ) has three type of carbons;  $\text{CH}$ ,  $\text{CH}_2$  and quaternary carbon atoms. The number of carbons is not coincide with the molecular weight obtained from MS ( $m/z = 462$ ) which may be attributed to the similarity of some parts of the compound and overlapping of signal peaks. The compound showed the presence of aromatic protons at 6.6 to 7.2 ppm. The aromatic protons showed more overlapping indicating more than phenyl group and from the mass spectrum; we can expect three phenyl groups.  $^{13}\text{C}$  NMR and DEPT (90, 135) showed eight signals which don't agree with the mass structure indicating overlapping in some signals. It show two carbonyl group at 170.34 and 173.95 ppm, four signals of aromatic moiety at 112.76, 118.97, 129.01 and 149.52 ppm. There is a signal of a quaternary carbon atom at 75.22 ppm, which may attributed to the attachment of OH group at this carbon atom.

### 2D NMR spectrum

HSQC spectrum has been recorded for  $\text{H}_3\text{L}$  and it was used to assign the signals unambiguously. The correlations between carbons and hydrogen atoms was assigned by HSQC spectrum. Quaternary carbons do not show any correlation in the HSQC spectrum. HSQC shows correlation of a carbon signal at 41.12 ppm with two proton signals at 2.73 ppm. Three aromatic carbons at 112.76, 118.97 and 129.01 show correlations with protons at 6.77, 6.56 and 7.08 respectively. From the previous correlations, we can deduce that the aromatic moiety is monosubstituted phenyl ring. The phenyl ring is repeated three times in the structure to coincide with mass measurements. There is no correlation of the two down field carbons at 170.37 and 173.95 ppm indicating they may be carbonyl carbon. H N HSQC shows three protons at 7.52, 6.56 and 7.72 ppm are correlated to three nitrogen at 87.00, 87.50 and 89.00 ppm, which are typical of NH of aniline moiety[19]. In addition, there are other protons at 9.68, 9.75 and 9.81 are correlated to 3 nitrogen atoms at 139.0, 132.5 and 138.5 ppm which are typical with NH of amide moiety[20]. H-C COSY shows the correlation between the protons at 7.13 with proton at 112.76 the proton at 7.13 with proton at 118.97 and proton at 6.77 with proton at 118.97. This indicates that the proton positions at phenyl group as shown in Fig 3. In HC COSY, There are correlations between the NH aniline proton at 7.72, 7.57 and 7.52 with NH amide proton at 9.81, 9.68 and 9.75 respectively which indicate the presence of phenyl carbohydrazide moiety[21] as shown in Fig 3. Moreover, the protons of the  $\text{CH}_2$  at 2.73 and 2.76 ppm are correlated to each other.

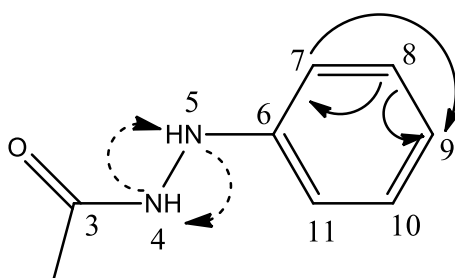


**Fig 3: The correlation between protons in HC COSY (solid arrows) and HH COSY (dotted arrows) in fragment A.**

HMBC shows correlations of protons of the two  $\text{CH}_2$  at 2.73 and 2.76 ppm with the carbon at 75.22 ppm, which may bearing OH group. From the previous findings, we can expect another new fragment **B**, 2-hydroxy propane moiety, as shown in Fig. 4.

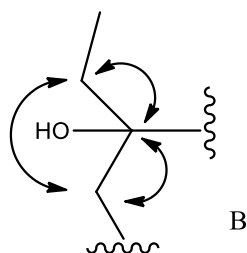


Fig 4: The other fragment as shown in HMBC

HMBC shows the correlations in the phenyl ring which confirm the ring is monosubstituted and showed the correlations between its protons and carbons as shown in Fig 5. From HMBC and HH COSY, the two fragments can be connected as shown in Fig 4. The correlation between the two CH<sub>2</sub> protons at 2.73 and 2.76 with NH protons at 9.81 and 9.68 at indicates that **H<sub>3</sub>L** has two of phenyl carbohydrazide moiety connected to 2hydroxy propane moiety through two the CH<sub>2</sub> group and the third phenyl carbohydrazide moiety connected to the propane moiety through the quaternary carbon bearing the hydroxyl group. This fragment did not show any correlation with CH<sub>2</sub> proton in HH COSY due to 4-bond length far. Another confirmation for the connection of fragment **A** and **B** is the correlation in HMBC between the two coincide carbonyl carbon at 170.34 ppm with protons of CH<sub>2</sub> at 2.73 and 2.76. The Correlations as revealed from HH COSY and HMBC is shown in Fig 5.

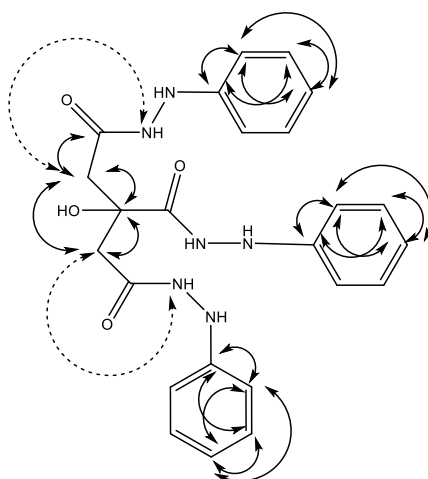


Fig 5: HMBC (solid arrows) and H H COSY (dotted arrows) correlation

## INFRARED SPECTRA

The ligand infrared spectrum revealed a strong peaks observed at 1698, 1683 and 1655 cm<sup>-1</sup> which can be ascribed to  $\nu(\text{C}=\text{O})$  groups of carboxylate moieties, whereas the medium bands appeared at 3323, 3288, 3260 cm<sup>-1</sup> assigned to the  $\nu(\text{OH})$  and  $\nu(\text{NH})$  groups. These observations confirmed that in the solid state, the carbohydrazide exhibits only the keto form[22]. The spectrum of the ligand also showed relatively week peaks at 3096, 3049 and 2951 cm<sup>-1</sup> assigned to the aromatic and aliphatic hydrogen of phenyl and propane moieties respectively. By comparison complexes infrared spectra with that of the ligand, it was found that, the bands characteristic to the carbonyl groups  $\nu(\text{C}=\text{O})$  disappeared. The disappearing of these peaks suggested that, the carbohydrazide bonded to the metal ions in its enolic form. This result is proposed by the appearing of new peaks in the 1557–1598 cm<sup>-1</sup> and 1241–1314 cm<sup>-1</sup> ranges which can be ascribed to the  $\nu(\text{N}=\text{C}-\text{O})$  and  $\nu(\text{C}-\text{O})$  respectively. It is concluded that, the enolic carbonyl groups participate in the bonding to the metal ions as in complexes **(2)**, **(5-6)**, **(8-9)** and **(11-12)**. In complexes **(3-4)**, **(7)** and **(10)** the characteristic band of carbonyl group was shifted to lower wavenumber with remarkable decreasing its intensity indicating that in these complexes the carbonyl group participate in chelation in its ketonic form. The amine groups  $\nu(\text{NH})$  characteristic band was shifted slightly to lower frequency with decreasing their intensities indicating their coordination to the central metal ion. In the same time the distinctive band of the  $\nu(\text{N}-\text{N})$  which appeared in the spectra of the ligand at 1010 cm<sup>-1</sup> shifted to higher frequency and appearing in the range 1023–1063 cm<sup>-1</sup>

confirming the coordination of nitrogen atom to metal ions. The bands due to the hydroxyl group was observed almost at its original position indicating that is not involved in chelation. The appearing of new peaks in the 502–575 and 453–500  $\text{cm}^{-1}$  ranges for different complexes (**2-12**) are ascribed to the  $\nu(\text{M}-\text{O})$  or  $(\text{M}\leftarrow\text{O})$  and  $\nu(\text{M}\leftarrow\text{N})$  respectively[23]. These bands were taken as indication for chelation of the ligand with the metal were occurred by the C–O or C=O and C=N. IR spectra of the nitrate complexes (**3**), (**6**), (**9**) and (**12**) showed bands in the  $\nu_5(1435-1457)$ ,  $\nu_1(1361-1391)$  and  $\nu_2(901-922)$  ranges indicating the nitrate group bonded covalency to the metal ions. The differences between the two high bands ( $\nu_5-\nu_1$ ) are in the 63-90  $\text{cm}^{-1}$  indicating that, the nitrate ion bonded covalency to the metal ion is unidentate manner[24-25]. In sulfato complexes, the sulfate group may bind to the metal ions either as a unidentate ligand with  $C_{3v}$  local site symmetry or as a bidentate ligand with  $C_{2v}$  symmetry thus, it may act either as a chelating or a bridging ligand. Complexes involving monodentate sulfato ligands display splitting of the  $\nu_3$  and  $\nu_4$  ( $\text{SO}_4$ ) modes into two bands and ir-active  $\nu_1$  and  $\nu_2$  modes[24, 26]. This is the case of complex (**4**) which show bands at 1147, 1045 assigned to  $\nu_3$ , 966, 510 assigned to  $\nu_4$ , and 630, 594 assigned to  $\nu_1$  and  $\nu_2$  [24, 27]. In bidentate bridging or chelating sulfato complexes,  $\nu_3$  and  $\nu_4$  are split into three bands, while  $\nu_1$  and  $\nu_2$  are again ir-active. difference between chelating and bridging sulfato ligands is clear by the  $\nu_3$  bands positions; thus, complexes involving chelating bidentate sulfate demonstrate the three  $\nu_3$  absorptions at 1240-1000  $\text{cm}^{-1}$ , while those containing bridging bidentate sulfate show these bands at 1200-1030  $\text{cm}^{-1}$ . IR spectra of the complexes (**7**) and (**10**), revealed new bands in the ranges 1231-1240, 1100-1115 and 1032-1043  $\text{cm}^{-1}$  which assigned to the  $\nu_3$  supposing the sulphate group probably chelated to the central metal ions in a bidentate manner[24, 26]. In all complexes, the broadening appeared in high wavenumber region assigned to the presence of water molecules[28-29].

The above arguments together with elemental analysis indicate that the behavior of carbohydrazide ligand are neutral or tribasic hexadentate ligand toward three metal ions bonded or chelated to the central metal ions through the three-carbonyl oxygen atoms in ketonic or enolic forms and three nitrogen atoms of amine groups.

#### MASS SPECTRA

The ligand mass spectrum supports the suggested structure of the carbohydrazide. It reveals molecular ion peak  $m/z$  at 462 and proportionate with the molecular weight of the ligand.

#### MOLAR CONDUCTIVITY

The complexes molar conductance data, which are measured in DMSO solution at concentration of 0.001 M. The conductance values fall in the of 13.7-30.35  $\text{ohm}^{-1}\text{cm}^2\text{mol}^{-1}$  range, that is within the expected range of 1–35  $\text{ohm}^{-1}\text{cm}^2\text{mol}^{-1}$  for the complexes to act as nonelectrolytes.[30] Thus, these complexes have a non-electrolytic nature as evidenced by the involvement of the, chloride, nitrate and sulfate groups in coordination. The high values of some complexes could be attributed the partial solvolysis by solvent molecules.

#### ELECTRONIC SPECTRA AND MAGNETISM

The electronic absorption spectrum of the ligand in solid state showed that the ligand exhibits three bands at 219, 244 and 288 nm. The first one assigned to intraligand  $\pi\rightarrow\pi^*$  transition in the benzoniod moiety which nearly unchanged on complexation. The second and third bands may be as attributed to the  $n\rightarrow\pi^*$  transitions of the amine and carbonyl groups. These bands are shifted to longer wavelength on complexation denoting the sharing of these groups in coordination process[22, 31]. In addition, the complexes spectra revealed new bands appeared in the range 346–418 nm, which can be ascribed to the LMCT transitions[22, 31]. The absorption spectra of six-coordinate copper(II) complexes are analyzed supposing  $D_4$  or  $C_{4v}$  symmetry, the  $e_g$  and  $t_{2g}$  levels of the  $^2D$  free ion term are further split into  $B_{1g}$ ,  $A_1$ ,  $B_{2g}$  and  $E_g$  levels, respectively. Thus, three spin allowed transitions are predicted in the visible and near IR region of copper(II) ions which are resolved by Gaussian and single crystal polarization analysis. These bands are assigned to the  $(\nu_1)^2B_{1g}\rightarrow^2A_{1g}(d_{x^2-y^2}\rightarrow d_{z^2})$ ;  $(\nu_2)^2B_{1g}\rightarrow^2B_{2g}(d_{x^2-y^2}\rightarrow d_{xy})$  and  $(\nu_3)^2B_{1g}\rightarrow^2E_g(d_{x^2-y^2}\rightarrow d_{xz}, d_{yz})$  transitions in order of increasing energy. The energy level sequence will depend on the amount of distortion, due to ligand field and Jahn-Teller effect[32]. Copper(II) complex (**2**) showed three bands at 585, 670, 1055 nm assignable to  $(\nu_1)^2B_{1g}\rightarrow^2A_{1g}(d_{x^2-y^2}\rightarrow d_{z^2})$ ,  $(\nu_2)^2B_{1g}\rightarrow^2B_{2g}(d_{x^2-y^2}\rightarrow d_{xy})$  and  $(\nu_3)^2B_{1g}\rightarrow^2E_g(d_{x^2-y^2}\rightarrow d_{xz}, d_{yz})$  transitions. These

transitions can be suggested that these complex may be considered to have five-coordinate geometry [Fig. 1][33-34]. The copper(II) complex **(3)** electronic absorption spectra in nujl mull showed three bands at 625, 660, 695 nm which could be ascribed to  $(v_3)^2B_{1g} \rightarrow ^2E_g(d_{x^2-y^2} \rightarrow d_{xy})$ ,  $(v_2)^2B_{1g} \rightarrow ^2B_{2g}(d_{x^2-y^2} \rightarrow d_{yz}, d_{xz})$  and  $(v_1)^2B_{1g} \rightarrow ^2A_{1g}(d_{x^2-y^2} \rightarrow d_{z^2})$  transitions respectively. These absorption bands indicate that these complexes have tetragonally distorted octahedral geometry [Fig. 1][35-37]. However the copper(II) complex **(4)** spectrum showed two band at 515 and 698 nm assignable to  $(v_1)^2B_{1g} \rightarrow ^2A_{1g}(d_{x^2-y^2} \rightarrow d_{z^2})$ , and  $(v_2)^2B_{1g} \rightarrow ^2B_{2g}(d_{x^2-y^2} \rightarrow d_{xy})$  transitions respectively suggesting that this complex may be believed to have square-planar geometry [Fig. 2][38]. The solid copper(II) complexes  $\mu_{eff}$  values at 25 °C were in the 1.34-1.65 BM range [Table 1] which are consistent with one unpaired electron configuration. The low value of complexes are inductive to spin spin interaction between copper(II) ions through molecular association[25]. At room temperature Co(II) complexes **(5)** and **(6)** electronic spectra show electronic spectral bands at 1018, 580, 440 nm corresponding to the transitions  $^4T_{1g}(F) \rightarrow ^4T_{2g}(F)$ ,  $^4T_{1g}(F) \rightarrow ^4A_{2g}(F)$  and  $^4T_{1g}(F) \rightarrow ^4T_{1g}(P)$  suggesting a six coordinated octahedral geometry. The ratio of  $v_2/v_1$  is 1.755 which is lower than usual range for an octahedral cobalt(II) (1.95–2.48), indicates that these complex have distorted octahedral structure[37, 39-42]. However the cobalt complex **(6)** and **(7)** electronic spectra show three transitions at 440, 445; 580, 600 and 1059, 1030 which could be assigned to  $(v_1)^4A_2 \rightarrow ^4T_2$ ,  $(v_2)^4A_2 \rightarrow ^4T_1(F)$  and  $(v_3)^4A_2 \rightarrow ^4T_1(P)$  respectively indicating that the cobalt(II) ions have a tetrahedral structure[37, 43]. The solid cobalt(II) complexes  $\mu_{eff}$  values at 25 °C were in the 1.93-2.33 BM range [Table 1]. These values are lower than the expected to three unpaired electron configuration (3.87 BM). These low values may be due spin spin interaction between cobalt(II) ions ( $d^7$ ) through molecular association[25]. Ni(II) complexes are capable to form coordination compounds of different stereochemistry viz. square planar, tetrahedral, and octahedral. In an octahedral field, the 3F Russel–Saunders term split into three components  $^3A_{2g}$ ,  $^3T_{2g}$ , and  $^3T_{1g}$  in order of increasing energy.  $^1D$  splits into  $^1E_g$  and  $^1T_{2g}$ ,  $^3P$  changes into  $^3T_{1g}$ ,  $T_{2g}$  thus spin allowed transitions are possible. The electronic spectra of the nickel complex **(8)** are consistent with an octahedral stereochemistry around the nickel(II) ion, showing transition bands at 1041, 708, 559 nm. These are assignable to the transitions  $^3A_{2g}(F) \rightarrow ^3T_{2g}(F)$ ,  $^3A_{2g}(F) \rightarrow ^3T_{1g}(F)$ ,  $^3A_{2g}(F) \rightarrow ^3T_{1g}(P)$ , respectively [33, 37, 39, 44]. The  $v_2/v_1$  ratio of these complexes are 1.47 which is less than the usual range (1.50–1.75), inductive to distorted octahedral stereochemistry nickel(II) complexes[45]. However the nickel(II) complexes **(9)** and **(10)** electronic spectrum shows transition at 1051 and 557 nm corresponding to the  $^3A_2(F) \leftarrow ^3T_1(F)$  and  $^3T_1(P) \leftarrow ^3T_1(F)$  transitions, respectively, which are similar to those described in the literature for tetrahedral coordinated Ni(II) complexes[37, 46-48]. The solid Ni(II) complexes  $\mu_{eff}$  values at 25 °C were in the 1.69-2.49 BM range [Table 1]. These values are lower than expected to two unpaired electron configuration. These low values resulted from the spin spin interaction between nickel(II) ions through molecular association[25]. For Fe(III), there are three transitions:  $(v_1)^6A_{1g}(S) \rightarrow ^4T_{1g}(G)$ ,  $(v_2)^6A_{1g}(S) \rightarrow ^4T_{2g}(G)$  and  $(v_3)^6A_{1g}(S) \rightarrow ^4A_{1g}(G), ^4E_g(G)$ .  $v_1$  locates around  $950\text{ cm}^{-1}$ ,  $v_2$  occurs between  $650$  to  $550\text{ cm}^{-1}$  usually as a shoulder. However  $v_3$  appear around  $450\text{ cm}^{-1}$ [49]. The Fe(III) complexes **(11)** and **(12)** exhibit two absorption bands at 1041, 1021; 540, 589, 485, 500nm, which may be corresponded to  $v_1$ ,  $v_2$  and  $v_3$  transitions respectively, suggesting distorted octahedral geometry around the Fe(III) ions. The solid Fe(III) complexes  $\mu_{eff}$  values at 25 °C were 4.45 and 4.89 BM respectively [Table 1]. These values are lower than expected to high spin iron(III) configuration ( $d^5$ ). These low values may be resulted from the spin-spin interaction between iron(III) ions through molecular association[25].

**Table 1: UV-Vis. spectra of the ligand (HL) and its metal complexes**

No	Electronic transitions		Electronic transition	$\mu_{eff}(\text{BM})/M$	Geometry
	$\pi \rightarrow \pi^*$ , $n \rightarrow \pi$ , LMCT	d-d transitions			
1	219, 244, 288	--	---	--	--
2	222, 246, 321, 395	585, 670, 1055	$(v_3)^2B_{1g} \rightarrow ^2E_g(d_{x^2-y^2} \rightarrow d_{xz}, d_{yz})$ $(v_2)^2B_{1g} \rightarrow ^2B_{2g}(d_{x^2-y^2} \rightarrow d_{xy})$ $(v_1)^2B_{1g} \rightarrow ^2A_{1g}(d_{x^2-y^2} \rightarrow d_{z^2})$	1.29	five-coordinate geometry
3	220, 245, 280, 380	625, 660, 695	$(v_3)^2B_{1g} \rightarrow ^2E_g(d_{x^2-y^2} \rightarrow d_{xy})$ , $(v_2)^2B_{1g} \rightarrow ^2B_{2g}(d_{x^2-y^2} \rightarrow d_{yz}, d_{xz})$ $(v_1)^2B_{1g} \rightarrow ^2A_{1g}(d_{x^2-y^2} \rightarrow d_{z^2})$	1.34	tetragonal distorted octahedral
4	230, 257, 269, 418	515, 698	$(v_2)^2B_{1g} \rightarrow ^2B_{2g}(d_{x^2-y^2} \rightarrow d_{yz}, d_{xz})$ $(v_1)^2B_{1g} \rightarrow ^2A_{1g}(d_{x^2-y^2} \rightarrow d_{z^2})$	1.65	Square planar

5	225, 249, 280, 380	440, 580, 1018	$(\nu_3)^4T_{1g}(F) \rightarrow ^4T_{1g}(P)$ $(\nu_2)^4T_{1g}(F) \rightarrow ^4A_{2g}(F)$ $(\nu_1)^4T_{1g}(F) \rightarrow ^4T_{2g}$	1.93	distorted octahedral
6	228, 248, 316	459, 646, 1059	$(\nu_1)^4A_2 \rightarrow ^4T_2$ $(\nu_2)^4A_2 \rightarrow ^4T_1(F)$	2.16	tetrahedral
7	222, 260, 320	445, 600, 1030	$(\nu_3)^4A_2 \rightarrow ^4T_1(P)$	2.33	
8	223, 244, 290, 400	559, 708, 1041	$(\nu_3)^3A_{2g}(F) \rightarrow ^3T_{1g}(P)$ $(\nu_2)^3A_{2g}(F) \rightarrow ^3T_{1g}(F)$ $(\nu_1)^3A_{2g}(F) \rightarrow ^3T_{2g}(F)$	2.49	distorted octahedral
9	220, 311, 420	580, 1026	$^3A_2(F) \rightarrow ^3T_1(F)$	1.86	tetrahedral
10	234, 277, 346	577, 1051	$^3T_1(P) \rightarrow ^3T_1(F)$	1.69	
11	227, 246, 326, 364	485, 1041	$(\nu_1)^4A_{1g}(S) \rightarrow ^4T_{1g}(G)$ $(\nu_2)^4A_{1g}(S) \rightarrow ^4T_{2g}(G)$	4.45	Distorted octahedral
12	236, 311, 350	500, 1021	$(\nu_3)^4A_{1g}(S) \rightarrow ^4A_{1g}(G) \ ^4E_g(G)$	4.89	

### THERMAL ANALYSES OF SOME COMPLEXES

The thermogravimetric analyses (TG) of complexes **(2-5)**, **(8)** and **(10-11)** were performed within temperature range 20–800 °C to give an insight into the thermal stability and the nature of water molecule of the studied complexes. The TG data revealed that the calculated weight loss agree with the suggested formulae. The complexes **(2-4)**, **(8)** and **(11)** show weight loss in three notable stages (Table 2). In the first stage losing in weight take place within 115-270 °C range are expt: 11.63, 5.77, 4.99, 17.67 and 10.90 %; theo: 12.50, 6.07, 5.43, 17.93 and 11.40 % respectively complies with loss of six, nine or three water molecules. The losing of weight in the second stage are expt: 12.00, 31.23, 28.34, 11.55 and 38.87 %; theo: 12.30, 32.83, 28.93, 11.76 and 39.25 % respectively that occur in the 220-350 °C range complies to the losing of three HCl, six HNO<sub>3</sub> or three H<sub>2</sub>SO<sub>4</sub> molecules. [28], while the percentage weight loss in the 350-765 °C range complies the completely degradation of the complexes molecules.

**Table 2: The thermal analysis (TG) of some complexes**

No.	Temp. range °C	Loss in weight Found (calcd.)	assignment	Composition of the residue
2	145-200	11.63 (12.50)	Loss of coordinated water molecule (6H <sub>2</sub> O)	[Cu <sub>3</sub> (L)(Cl) <sub>3</sub> ]
	220-350	12.00(12.30)	Loss of three chloride ions (3HCl)	[Cu <sub>3</sub> (L)]
	350-680	63.77(65.99)	Complex decomposition forming CuO	3CuO
3	135-270	5.77 (6.07)	Loss of coordinated water molecule (6H <sub>2</sub> O)	[Cu <sub>3</sub> (H <sub>3</sub> L)(NO <sub>3</sub> ) <sub>6</sub> ]
	300-350	31.23(32.83)	Loss of six nitrate ions (6HNO <sub>3</sub> )	[Cu <sub>3</sub> (H <sub>3</sub> L)]
	420-710	48.99 (50.61)	Complex decomposition forming CuO	3CuO
4	120-190	4.99 (5.43)	Loss of coordinated water molecule (3H <sub>2</sub> O)	[Cu <sub>3</sub> (H <sub>3</sub> L)(SO <sub>4</sub> ) <sub>3</sub> ]
	230-290	28.34 (28.93)	Loss of three sulfate ions (3H <sub>2</sub> SO <sub>4</sub> )	[Cu(L)]
	370-600	55.04(57.65)	Complex decomposition forming CuO	3CuO
5	70-110	8.22 (7.38)	Dehydration process (4H <sub>2</sub> O)	[Co <sub>3</sub> (L)(Cl) <sub>3</sub> (H <sub>2</sub> O) <sub>9</sub> ]
	135-215	15.68 (16.60)	Loss of coordinated water molecule (9H <sub>2</sub> O)	[Co <sub>3</sub> (L)(Cl) <sub>3</sub> ]
	255-295	10.35 (10.89)	Loss of three chloride ions (3HCl)	[Co <sub>3</sub> (L)]
	390-655	55.99 (57.47)	Complex decomposition forming CoO	3CoO
8	115-230	17.67 (17.93)	Loss of coordinated water molecule (9H <sub>2</sub> O)	[Ni <sub>3</sub> (L)(Cl) <sub>3</sub> ]
	245-275	11.55(11.76)	Loss of three chloride ions (3HCl)	[Ni <sub>3</sub> (L)]
	370-665	61.39(62.04)	Complex decomposition forming NiO	3NiO
10	190-315	29.66 (31.07)	Loss of three sulfate ions (3H <sub>2</sub> SO <sub>4</sub> )	[Ni <sub>3</sub> (H <sub>3</sub> L)]
	380-570	58.97(60.87)	Complex decomposition forming NiO	3NiO
11	125-230	10.90 (11.40)	Loss of coordinated water molecule (6H <sub>2</sub> O)	[Fe <sub>3</sub> (L)(Cl) <sub>6</sub> ]
	250-280	38.87 (39.25)	Loss of six chloride ions (6HCl)	[Fe <sub>3</sub> (L)]
	350-765	37.66(40.92)	Complex decomposition forming Fe <sub>2</sub> O <sub>3</sub>	1.5Fe <sub>2</sub> O <sub>3</sub>

The complexes  $[Co_3(L)(Cl)_3(H_2O)_9].4H_2O$  (**5**) shows essentially weight loss in four notable stages (Table 2). The first stage, the weight loss equal to 8.22 % which occur in the 65-120 °c ranges complies to the elimination of four water molecules of hydration (theo: 7.38 %), respectively. The loss of nine water molecules in the 130–230 °c range in these complexes may be indicated the presence of water molecules in the coordination sphere of these complexes. However, these complexes show third stage of degradation in the 250-295 °c range with weight loss expt: 10.35 and 11.55 %; theo: 10.89 and 11.76 % respectively which may be ascribed to the elimination of three HCl molecules. The last stage of degradation of these complexes occur in the 370-665 °c range with weight loss equal to expt: 55.99 and 61.39 %; theo: 57.47 and 62.04 % respectively which may be attributed to the completely degradation of the complexes molecules leaving residue as metal oxide. TG data of complex (**10**) suggests that this complex shows two stage of degradation. The first stage take place in the 190-315 °c range with losing of weight equal to expt: 29.66 %; theo: 31.07 % complies to loss of three H<sub>2</sub>SO<sub>4</sub> molecules. While the percentage weight loss in the 380-570 °c range complies the complete degradation of the complexes molecules with formation of NiO.

**ANTIMICROBIAL SCREENING**

All complexes were subjected to antifungal and antibacterial screening tests against fungi as *A. niger* and bacteria like *E. coli*, *K. pneumonia*. The screening data are summarized in Table 3. The complexes exhibited higher antifungal and antibacterial activities than the free ligand. However, the complexes are more active against fungi than bacteria. The MIZ values revealed that complexes (**5**) and (**9-10**) exhibit antifungal activity against *A. niger* (MZI = 34(136%), 29(116%) and 35(140%) mm (activity Index %) respectively) more than that observed for antifungal drug, Nystatin, MZI = 25, Table 3. Moreover, the other complexes have moderate antifungal activity with MIZ in the 11-21 mm and activity index ranged from 40% to 84%, in comparing to antifungal drug, Nystatin.

**Table 3: Biological activities of the ligand and its metal complexes against *A. niger*, *E. coli* and *K. Pneumonia***

No.	Inhibition zone (mm) and Activity Index (%)					
	<i>A. niger</i>	Activity Index (%)	<i>E. coli</i>	Activity Index (%)	<i>K. Pneumonia</i>	Activity Index (%)
DMSO	0	0%	0	0%	0	0%
Nystatin	25	100%	--	0%	--	--
Amoxicillin	--	--	34	100%	43	100%
<b>1</b>	10	40%	10	29%	9	21%
<b>2</b>	11	44%	13	38%	19	44%
<b>3</b>	12	48%	16	47%	10	23%
<b>4</b>	17	68%	18	53%	10	23%
<b>5</b>	34	136%	20	59%	21	49%
<b>6</b>	19	76%	18	53%	9	21%
<b>7</b>	10	40%	10	29%	17	40%
<b>8</b>	14	56%	18	53%	15	35%
<b>9</b>	29	116%	11	32%	21	49%
<b>10</b>	35	140%	9	26%	27	63%
<b>11</b>	20	80%	10	29%	14	33%
<b>12</b>	21	84%	12	35%	18	42%

Otherwise, the antibacterial screening data reveled that all complexes have a weak activities against *E. coli* and *K. pneumonia* with MIZ values in the 13-21 and 10-27 mm ranges and activity index in the 29-59 and 21-63% ranges in comparing to antibacterial drug Amoxicillin. The enhancement in the potent antifungal and antibacterial activities of the complexes seems to be due to increment of lipophilic character of these

complexes which could be explained based on Overtone's concept[50-51] and Tweedy's Chelation theory[51-52]. Based on Overtone's concept of cell permeability, the liposolubility is an important factor in which the lipid material can pass through the lipid cell membrane, which manages the antifungal activity. The positive charge on the metal ion decreased largely due to electron donor groups on the ligand as well as overlap with ligand orbitals, which cause a decrease in the metal ion polarity. Furthermore, the lipophilicity can be enhanced by increasing the delocalization of  $\pi$ -electrons over the ligand rings. This lead to enhance the complex penetration through the cell membrane and blocking of the metal binding sites in the enzymes of microorganisms. As a result, deactivate various cellular enzymes, which play an important role in metabolic pathways of these microorganisms. It is also suggested that the function of the toxicant is the product of natural analogue of one or more proteins of the cell, which as a result, impairs the normal cellular processes.

### CONCLUSIONS

In this study we have reported the characterization of synthetic homotrimetallic Fe(II), Co(II) Ni(II) and Cu(II) complexes with an hexadentate  $N_3O_3$  carbohydrazide ligand analytically and spectroscopically. The geometries around the metal ions are distorted octahedral or tetrahedral. The in vitro antimicrobial activity of synthetic metal complexes were investigated. Antimicrobial screening tests showed that the complexes have exhibit higher antifungal and antibacterial activities than the free ligand. However, the complexes are more active against fungi than bacteria. The data revealed that the complexes (5) and (9-10) exhibit antifungal activity against *A. niger* more than that observed for antifungal drug, Nystatin.

### REFERENCES

- [1] Kirillov AM, Kirillova MV, Pombeiro AJL. Coordination Chemistry Reviews. 2012; 256: 2741-2759.
- [2] Gupta KC, Sutar AK. Coordination Chemistry Reviews. 2008; 252: 1420-1450.
- [3] Uchida N, Miyazaki T, Matsushita Y, Sameshima K, Kanayama T. Thin Solid Films. 2011; 519: 8456-8460.
- [4] Iguchi H, Nafady A, Takaishi S, Yamashita M, Bond AM. Inorganic Chemistry. 2014; 53: 4022-4028.
- [5] Wang S, Ding X-H, Li Y-H, Huang W. Coordination Chemistry Reviews. 2012; 256: 439-464.
- [6] Swavey S, Swavey R. Coordination Chemistry Reviews. 2009; 253: 2627-2638.
- [7] Korybut-Daszkiewicz B, Bilewicz R, Woźniak K. Coordination Chemistry Reviews. 2010; 254: 1637-1660.
- [8] Nakano M, Oshio H. Chemical Society Reviews. 2011; 40: 3239-3248.
- [9] Żurowska B. Inorganica Chimica Acta. 152-136 :418 ;2014 .
- [10] Solomon SS, Srikrishnan AK, Vasudevan CK, Anand S, Kumar MS, Balakrishnan P, Mehta SH, Solomon S, Lucas GM. Clinical Infectious Diseases. 2014; 59: 589-595.
- [11] Kumar MS, Rajanna KC, Venkanna P, Venkateswarlu M, Sudhakar Chary V .Synthesis and Reactivity in Inorganic, Metal-Organic and Nano-Metal Chemistry. 2016; 46: 642-646.
- [12] Vigato PA, Tamburini S, Fenton DE. Coordination Chemistry Reviews. 1990; 106: 25-170.
- [13] Zanello P, Tamburini S, Vigato PA, Mazzocchin GA. Coordination Chemistry Reviews. 1987; 77: 165-273.
- [14] Brooker S. Coordination Chemistry Reviews. 2001; 222: 33-56.
- [15] Gupta LK, Chandra S. Spectrochimica Acta - Part A: Molecular and Biomolecular Spectroscopy. 2008; 71: 496-501.
- [16] Vigato PA, Tamburini S. Coordination Chemistry Reviews. 2004; 248: 1717-2128.
- [17] Atwood DA, Harvey MJ. Chemical Reviews. 2001; 101: 37-52.
- [18] Mroziński J. Coordination Chemistry Reviews. 2005; 249: 2534-2548.
- [19] Li L, Zhang L, Lan Y, Zhang C. Magnetic Resonance in Chemistry. 747-744 :46 ;2008 .
- [20] Rule GS, Hitchens TK, Fundamentals of Protein NMR Spectroscopy, 2006 ed., Springer Science & Business Media, The Netherland, 2006.
- [21] Venkatachalam TK, Pierens GK, Reutens DC. Magnetic Resonance in Chemistry. 2014; 52: 98-105.
- [22] Gup R, Kirkan B. Spectrochimica Acta - Part A: Molecular and Biomolecular Spectroscopy. 2005; 62: 1188-1195.
- [23] Sallam SA, Orabi AS, El-Shetary BA, Lentz A. Transition Metal Chemistry. 2002; 27: 447-453.
- [24] Nakamoto K, Infrared and Raman Spectra of Inorganic and Coordination Compounds Part B: Applications in Coordination, Organometallic, and Bioinorganic Chemistry, 6th ed., John Wiley & Sons INC, USA, 2009.
- [25] Katsoulakou E, Bekiari V, Raptopoulou CP, Terzis A, Lianos P, Manessi-Zoupa E, Perlepes SP. Spectrochimica Acta - Part A: Molecular and Biomolecular Spectroscopy. 2005; 61: 1627-1638.

- [26] Karayannis NM, Mikulski CM, Pytlewski LL, Labes MM. *Inorganica Chimica Acta*. 1974; 10: 97-102.
- [27] Papatriantafyllopoulou C, Raptopoulou CP, Terzis A, Janssens JF, Perlepes SP, Manessi-Zoupa E. *Zeitschrift fur Naturforschung - Section B Journal of Chemical Sciences*. 2007; 62: 1123-1132.
- [28] Gudasi KB, Vadavi RS, Shenoy RV, Patil SA, Nethaji M. *Transition Metal Chemistry*. 2006; 31: 374-381.
- [29] Narang KK, Singh VP. *Transition Metal Chemistry*. 1996; 21: 507-511.
- [30] Geary WJ. *Coordination Chemistry Reviews*. 1971; 7: 81-122.
- [31] Maurya MR, Agarwal S, Bader C, Rehder D. *European Journal of Inorganic Chemistry*. 2005; 147-157.
- [32] Chanu OB, Kumar A, Ahmed A, Lal RA. *Journal of Molecular Structure*. 2012; 1007: 257-274.
- [33] Sathyanarayana DN, *Electronic absorption spectroscopy and related techniques*, Orient BlackSwan Universities press, India, 2001.
- [34] Bhattacharyya S, Kumar SB, Dutta SK, Tiekink ERT, Chaudhury M. *Inorganic Chemistry*. 1996; 35: 1967-1973.
- [35] Sreeja PB, Kurup MRP, Kishore A, Jasmin C. *Polyhedron*. 2004; 23: 575-581.
- [36] Qing-bao S, Zhong-lin L, Xiao-li W, Yong-xiang M. *Transition Metal Chemistry*. 1994; 19: 503-505.
- [37] Lever ABP, *Inorganic electronic spectroscopy*, Elsevier science, Amsterdam 1984.
- [38] Angelusiu M, Negoiu M, Bărbuceanu SF, Rosu T. *Revista de Chimie*. 2008; 59: 726-729.
- [39] Xiao-Hui S, Xiao-Zeng Y, Cun L, Ren-Gen X, Kai-Be Y. *Transition Metal Chemistry*. 1995; 20: 191-195.
- [40] Chandra S, Kumar A. *Spectrochimica Acta - Part A: Molecular and Biomolecular Spectroscopy*. 2007; 68: 1410-1415.
- [41] Chandra S, Sharma S. *Transition Metal Chemistry*. 2007; 32: 150-154.
- [42] El-Tabla AS, El-Bahnasawy RM, Shakdofa MME, Ibrahim Hamdy AEDA. *Journal of Chemical Research*. 2010; 88-91.
- [43] Syamal A. *ZAAC - Journal of Inorganic and General Chemistry*. 1976; 419: 189-192.
- [44] Ibrahim MM, Mersal GAM, Al-Juaid S, El-Shazly SA. *Journal of Molecular Structure*. 2014; 1056-1057: 166-175.
- [45] El-Tabl AS, Aly FA, Shakdofa MME, Shakdofa AME. *Journal of Coordination Chemistry*. 2010; 63: 700-712.
- [46] Fernández-Souto P, Romero J, García-Vázquez JA, Sousa A, Pérez-Lourido P, Valencia L. *Inorganic Chemistry Communications*. 2012; 26: 28-30.
- [47] Sutton D, *Electronic spectra of transition metal complexes*, McGraw-Hill, London, New York, 1968.
- [48] Satyanarayana S, Nagasundara KR. *Synthesis and Reactivity in Inorganic and Metal-Organic Chemistry*. 2004; 34: 883-895.
- [49] Reddy SL, Endo T, Reddy GS, *Electronic Absorption Spectra of 3d Transition Metal Complexes, Advanced Aspects of Spectroscopy*, InTech2012.
- [50] Anjaneyulu Y, Rao RP. *Synthesis and Reactivity in Inorganic and Metal-Organic Chemistry*. 1986; 16: 257-272.
- [51] Joseyphus RS, Nair MS. *Mycobiology*. 98-93 :36 ;2008 .
- [52] Dharmaraj N, Viswanathamurthi P, Natarajan K. *Transition Metal Chemistry*. 2001; 26: 105-109.
- [53] Svehla G, *Vogel's textbook of macro and semi micro Quantitative inorganic analysis*, 5th ed., Longman New York, 1979.
- [54] Welcher F. *Princeton, Von Nostrand*. 1958.
- [55] Vogel A, *A Text Book of Quantitative Inorganic Analysis*, ELBS, London, 1978.
- [56] Holzbecher Z, Divis L, Kral M, *Handbook of organic reagents in inorganic analysis, Handbook of organic reagents in inorganic analysis*, John Wiley1976.
- [57] Figgis B, Lewis J, Wilkins R. *Interscience*, New York. 1960; 403.
- [58] Du Toit EA, Rautenbach M. *Journal of Microbiological Methods*. 2000; 42: 159-165.
- [59] Akbar Ali M, Mirza AH, Yee CY, Rahgeni H, Bernhardt PV. *Polyhedron*. 2011; 30: 542-548.
- [60] Balouiri M, Sadiki M, Ibsouda SK. *Journal of Pharmaceutical Analysis*. 2016; 6: 71-79.
- [61] Holder IA, Boyce ST. *Burns*. 1994; 20: 426-429.